Journal of Experimental Nanoscience
Publication details, including instructions for authors and subscription information:
http://www.informaworld.com/smpp/title~content=t716100757

Syntheses and characterisation of silver nanoparticles in the acrylate copolymers

S. Usha Rani[a]; K. Jeeva Pandian[b]; Boreddy S. R. Reddy[c]
[a] Department of Chemistry, SIVET College, Chennai 600073, Tamil Nadu, India [b] Department of Inorganic chemistry, Madras University, Chennai 600025, Tamil Nadu, India [c] Industrial Chemistry Laboratory, Central Leather Research Institute, Chennai 600020, Tamil Nadu, India

To cite this Article Usha Rani, S. , Jeeva Pandian, K. and Reddy, Boreddy S. R.(2009) 'Syntheses and characterisation of silver nanoparticles in the acrylate copolymers', Journal of Experimental Nanoscience, 4: 4, 285 — 299
To link to this Article: DOI: 10.1080/17458080903115338
URL: http://dx.doi.org/10.1080/17458080903115338

Journal of Experimental Nanoscience
Vol. 4, No. 4, December 2009, 285–299

Syntheses and characterisation of silver nanoparticles in the acrylate copolymers

S. Usha Rani[a], K. Jeeva Pandian[b] and Boreddy S.R. Reddy[c]*

[a]*Department of Chemistry, SIVET College, Chennai 600073, Tamil Nadu, India;* [b]*Department of Inorganic chemistry, Madras University, Guindy Campus, Chennai 600025, Tamil Nadu, India;* [c]*Industrial Chemistry Laboratory, Central Leather Research Institute, Adyar, Chennai 600020, Tamil Nadu, India*

(*Received 12 August 2008; final version received 13 June 2009*)

Silver nanoparticles were synthesised by polyol method using copolymer templates under microwave heating. The copolymer templates were synthesised by reacting the synthesised macromonomers with comonomer using free radical polymerisation. The copolymers were characterised by Fourier Transform InfraRed, ^{1}H-NMR and ^{13}C-NMR. The copolymers were further characterised by gel permeation chromatography for molecular weights and thermogravimetric analysis for thermal stability. These copolymers were used as nanoreactors in the syntheses of silver nanoparticles. The nanoparticles were characterised by various instrumental methods like UV-visible, FT-IR and High-resolution transmission electron microscopy to establish the average particle size and shape. Antibacterial activities of the copolymer-stabilised silver nanoparticles were tested on various microorganisms.

Keywords: syntheses; characterisation; copolymer templates/nanoreactors; microwave irradiation; silver nanoparticles; anti-bacterial activity

1. Introduction

Recent developments in the nanoscale materials have opened up a new opportunity for the building of functional nanostructures. The value and the benefit that the nanoparticles are expected to impart in different applications commercially demand that they be produced cost effectively on a large scale.

An economically viable process, capable of producing metal nanoparticles encapsulated in the polymers, is of prime importance. Generally, a polymer that effectively complexes the metal atom is preferred as it prevents agglomeration and therefore a direct kinetic control over the shape and size of the metal nanoparticles is achieved. The polymer functions as stabiliser/capping agent/template or as a nanoreactor in the growth of the

---

*Corresponding author. Email: induchem2000@yahoo.com

ISSN 1745–8080 print/ISSN 1745–8099 online

DOI: 10.1080/17458080903115338
http://www.informaworld.com

metal nanoparticles. Linear polymers like poly (vinyl pyrrolidone), poly (vinyl alcohol), poly (acrylic acid) and their copolymers, poly (amido amine), poly (acrylonitrile) and poly (acrylamide) were widely used templates in the synthesis of metal nanoparticles [1–7]. The present investigation involves the usage of acrylate copolymers as templates. This method provides a facile route for the large-scale production of silver nanoparticles. Systematic studies on the influence of several parameters in the synthesis of silver nanoparticles under various experimental conditions were reported.

2. Experimental

2.1. *Materials*

Silver acetate, silver nitrate, styrene and all the solvents used were of analytical grade. All other chemicals used were received from commercial sources.

2.2. *Synthesis of the copolymer*

The copolymers [copoly(S-7MPEGA), copoly(S-5MPEGA) and copoly(S-3MPEGA] were prepared and characterised. As an illustrative example the synthesis of copoly(S-7MPEGA) is described below. Copolymerisation was carried out with comonomer styrene and macromonomer 7MPEGA [the macromonomers were synthesised as reported in the literature]. Five copolymers with different compositions were synthesised using benzoyl peroxide as a free radical initiator in DMF medium at 70 ± 1°C in a polymerisation tube, purged with nitrogen gas and heated in an oil bath over a period of 24 h. To this polymer solution, *n*-hexane was added to dissolve any unreacted monomers and the solvent was then removed by distillation under reduced pressure. FT-IR, ^{1}H-NMR and ^{13}C-NMR spectral data then characterised the resulting copolymer solution.

Characterisation of copoly(S-7MPEGA): IR [ν, cm^{-1}]: (aro.C–H str.) 3030 cm^{-1}, (C–H str.) 2875 cm^{-1}, (sat.ester) 1717 cm^{-1}, (aro.C=C bend) 1667–1452 cm^{-1}, (C–H bend) 1408–851 cm^{-1}, (C–O str.) 1292 cm^{-1}, (C–C str.) 1108 cm^{-1}, (aro.C–H bend) 952–661 cm^{-1}. ^{1}H-NMR [300 MHz, CDCl$_3$, δ, ppm]: (s, 64H, (–OCH$_2$CH$_2$–)$_{16}$) 3.53δ and (s, 5H, aro.protons. sty) 7.97δ. ^{13}C-NMR [300 MHz, CDCl$_3$, δ, ppm]: C4 (163), C7–C10 (128–132), C2, C3 (69–71), C1 (69), C5 (36) and C6 (31).

Characterisation of copoly(S-5MPEGA): IR [ν, cm^{-1}]: (aro.C–H str.) 3439 cm^{-1}, (C–H str.) 2914 cm^{-1}, (sat.ester) 1718 cm^{-1}, (aro.C=C bend) 1666–1453 cm^{-1}, (C–H bend) 1453–848 cm^{-1}, (C–O str.) 1253 cm^{-1}, (C–C str.) 1105 cm^{-1}, (aro.C–H bend) 952–661 cm^{-1}. ^{1}H-NMR (300 MHz, CDCl$_3$, δ, ppm): (s, 35H, (–OCH$_2$CH$_2$–)$_{11}$) 3.59δ and (s, 5H, aro.protons. sty) 7.97δ. ^{13}C-NMR (300 MHz, CDCl$_3$, δ, ppm): C4 (166.2), C7–C10 (128–131), C2, C3 (70.5–71.9), C1 (63.7), C5 (36.6) and C6 (31.5).

Characterisation of copoly(S-3MPEGA): IR [ν, cm^{-1}]: (aro.C–H str.) 3440 cm^{-1}, (C–H str.) 2922 cm^{-1}, (sat.ester) 1727 cm^{-1}, (aro.C=C bend) 1668–1450 cm^{-1}, (C–H bend) 1450–852 cm^{-1}, (C–O str.) 1254 cm^{-1}, (C–C str.) 1099 cm^{-1}, (aro.C–H bend) 950–661 cm^{-1}. ^{1}H-NMR [300 MHz, CDCl$_3$, δ, ppm]: (s, 28H, (–OCH$_2$CH$_2$–)$_7$) 3.53δ and (s, 5H, aro.protons. sty) 7.97δ. ^{13}C-NMR [300 MHz, CDCl$_3$, δ, ppm]: C4 (166.6), C7–C10 (128.2–130.1), C2, C3 (70.4–71.8), C1 (58.9), C5 (36.5) and C6 (31.4).

2.3. *Synthesis of the silver nanoparticles in the copolymer template*

About a 30 mg sample of each of the copolymers with five different copolymer compositions was dissolved in 10 mg of the CH_3COOAg in 10 mL of DMF as a reducing agent. The reaction mixture was heated under microwave condition for 60 s. After the microwave irradiation, the colloidal solution obtained was characterised. A similar procedure was adopted by taking $AgNO_3$ instead of CH_3COOAg. The formations of silver nanoparticles were also monitored with different time intervals, namely 30 s, 60 s and 90 s. The resulting colloidal solution was then characterised by HRTEM, UV and FT-IR.

2.4. *Instrumentation*

Fourier Transform Infrared spectrometer: FT-IR spectra were collected on a Shimadzu FT-IR spectrometer and a neat solution was employed for the analysis. NMR spectrometer: ^1H and ^{13}C NMR spectrum were recorded on a Bruker-320 MHZ spectrometer at room temperature, using $CDCl_3$ as solvent. TMS was used as an internal standard. Thermogravimetric analysis: TGA of copolymer were recorded with 10–15 mg of samples at a heating rate of $10^\circ C\,min^{-1}$ under flowing high purity N_2. Gel permeation chromatography: GPC was performed using Shimadzu instrument. Tetrahydrofuran was used as the eluent at a flow rate of 0.3 $mL\,min^{-1}$ and polystyrene standards of different molecular weights were employed for calibration. Ultra-violet Visible absorption spectrophotometer: UV spectra were taken with a Tec-comp UV2300 spectrometer. The sample solutions were diluted using DMF and this dilute solution was put in a quartz cuvette of 1 cm optical path length for measurement. High-resolution transmission electron microscope: HRTEM was conducted by employing the model JEOL, JEM-3010, 300 KeV field emission transmission electron microscopy using an accelerating voltage of 200 KeV. The filament used was LaB_6. A drop of the suspension was placed onto a carbon-coated copper micro-grid a day prior to the observation. The excess solution was removed using a filter paper and the grid was then dried. The sample was examined by HRTEM and the TEM micrographs taken. Antibacterial activity: For antibacterial activity screening, the agar well diffusion method was used. DMF alone served as negative control and erythromycin ($5\,g\,mL^{-1}$) was used as positive control. Diameters of the zones of growth inhibition observed in the plates were measured using Hi-antibiotic zone scale^{TM}.

3. Results and discussion

The copolymers were prepared by reacting the macromonomer with the comonomer in DMF medium. Benzoyl peroxide was used as the initiator. The polymerisation reaction was carried out at $70 \pm 1^\circ C$ to give the copolymer (Scheme 1). The copolymer conversion was restricted to less than 10%. The synthesised copolymers were characterised.

The copolymer-stabilised silver nanoparticles were synthesised by microwave heating of each of the copolymer with silver acetate/silver nitrate in DMF (Scheme 2). The reaction was carried out under various experimental conditions such as synthesising the silver nanoparticles in different copolymer templates, changing the metal precursor and varying the exposure time to microwave heating and also by changing the solvent. The synthesised copolymer-stabilised silver nanoparticles were characterised by HRTEM, UV and FT-IR.

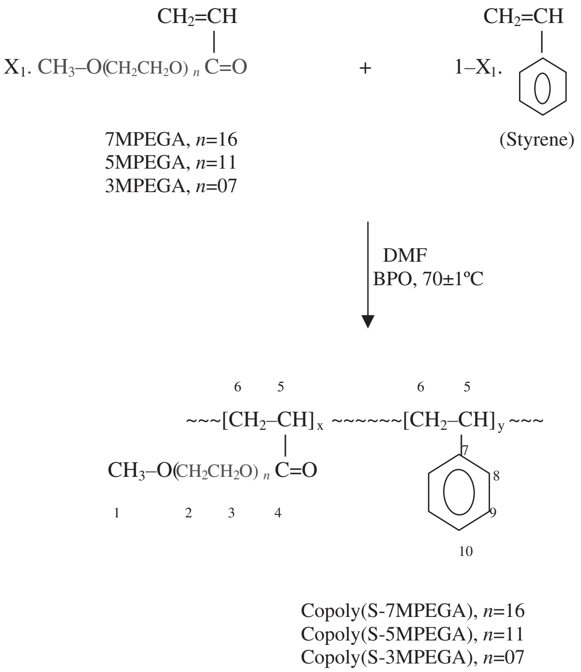

Scheme 1. Synthesis of copolymer.

3.1. *Characterisation of the copolymers*

The synthesised copolymers were characterised by IR, ^{1}H and ^{13}C NMR spectra.

3.1.1. *Thermal analysis*

Figure 1 represents the TGA curve for the copolymers of 50 : 50 compositions. The TGA data of the copolymers of 50 : 50 compositions regarding the weight loss percentage are presented in Table 1. The thermogravimetric analysis of the copolymers [namely, copoly(S-7MPEGA), copoly(S-5MPEGA), and copoly(S-3MPEGA) of 50 : 50 ratio exhibits the decomposition temperature to be around 351°C, 334°C and 324°C, respectively. The decomposition temperature increases with increasing molecular weight and hence is indicative of the thermal stability. Higher decomposition temperature suggests enhanced stability. A higher decomposition temperature of 351°C for copoly(S-7MPEGA) and a minimum of 324°C for copoly(S-3MPEGA) suggests that the copoly(S-7MPEGA) is highly stable while copoly(S-3MPEGA) is the least stable copolymer. Among the copolymers synthesised, the order of stability was found to be copoly(S-7MPEGA) > copoly(S-5MPEGA) > copoly(S-3MPEGA).

3.1.2. Gel permeation chromatography

The apparent molecular weights and polydispersity indices of the copolymers were determined by GPC in THF using polystyrene calibration. The ratio of weight-average molecular weight to number-average molecular weight (M_w/M_n) is indicative of the extent

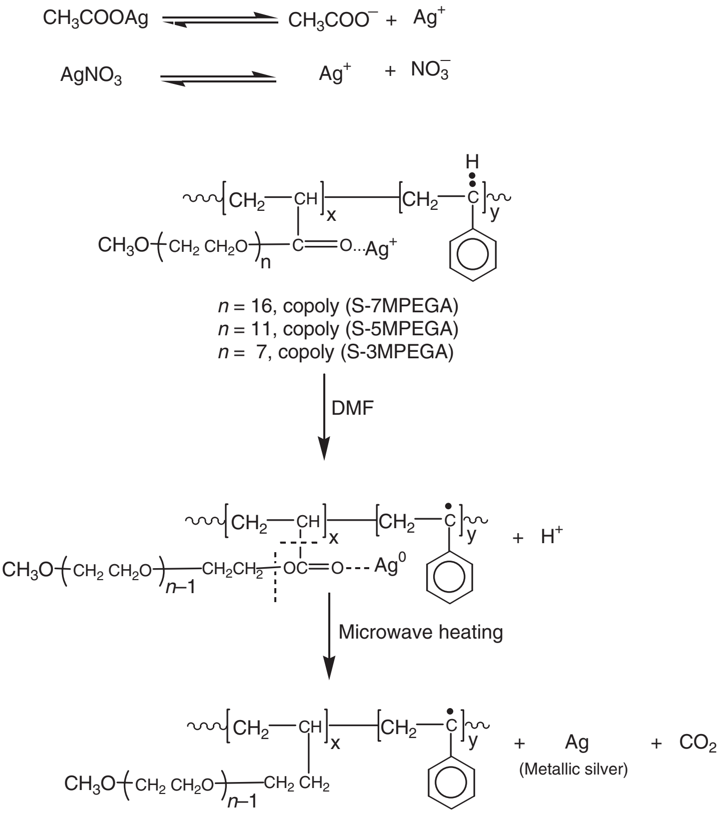

Scheme 2. Synthesis of silver nanoparticles.

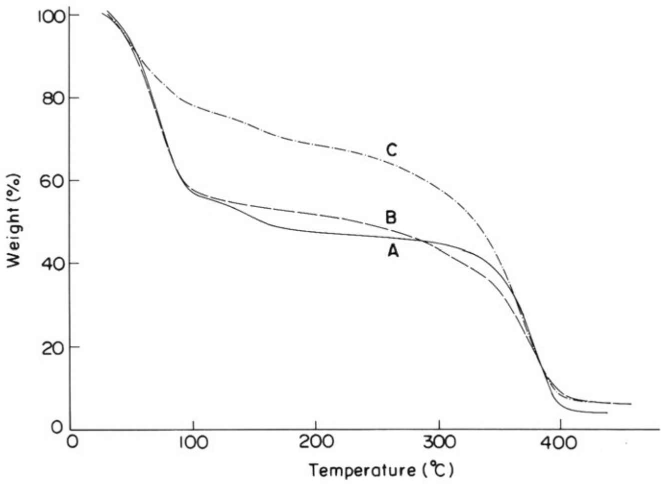

Figure 1. TGA plot for copolymers. (A) Copoly(S-7MPEGA), (B) copoly(S-5MPEGA), (C) copoly(S-3MPEGA).

Table 1. Thermal decomposition data of the copolymers.

Copolymer	Copolymer composition	Maximum decomposition temperature	Decomposition temperature for different % of weight loss								
			10%	20%	30%	40%	50%	60%	70%	80%	90%
Copoly(S-7MPEGA)	50 : 50	351	145	270	333	357	369	377	383	391	395
Copoly(S-5MPEGA)	50 : 50	334	140	185	276	344	358	370	378	388	398
Copoly(S-3MPEGA)	50 : 50	324	161	264	312	335	350	360	371	381	401

Table 2. Gel permeation chromatography.

Copolymers	Copolymer composition	Number-average molecular weight	Weight-average molecular weight	Polydispersity index
Copoly(S-7MPEGA)	50 : 50	2602	3006	1.155
Copoly(S-5MPEGA)	50 : 50	1920	2102	1.095
Copoly(S-3MPEGA)	50 : 50	1280	1540	1.203

of polydispersity. For all synthetic polymers, this ratio is higher than 1 and polymers obtained by different polymerisation techniques show different polydispersities. Synthetic copolymers obtained by free radical chain polymerisation with precise temperature control in solution, suspension and emulsion systems exhibit a polydispersity value of 1.5–2. A polydispersity value of 1.15, 1.89, 1.74, 1.66, 1.86, 1.77 and 1.93 was reported for copoly(MPEGA-S), copoly(EA-HPPMA), copoly(HEA-HPPMA), copoly(GMA-HPA), copoly(MA-HPPMA), copoly(NVP-HPPMA) and copoly(VC-HPPMA), respectively.

In the present investigation, the synthesised copolymers [namely, copoly(7MPEGA-S), copoly(5MPEGA-S) and copoly(3MPEGA-S)] also exhibit a polydispersity value of less than 2 as seen in Table 2, which is in accordance with the literature. Lower molecular weight and narrow poly dispersity index value suggest that highly mono-dispersed light weight polymers were formed [8–10].

3.2. *Characterisation of copolymer-stabilised silver nanoparticles*

3.2.1. *HRTEM*

Figure 2 shows the HRTEM micrograph of the silver nanoparticles encapsulated in copoly(S-7MPEGA) of composition 50 : 50 with 10 mg of CH_3COOAg in 10 mL of the DMF solution for 60 s under microwave conditions. Figure 2(a–e) reflects TEM images of the same sample obtained from the copoly(S-7MPEGA). The micrographs reveal that spherical or nearly spherical silver nanoparticles are formed. The particles are homogenously dispersed in the copolymer matrix. Each silver particle is well resolved and the morphology indicates that nanospheres are formed. In Figure 2(f), the histogram shows the particle size distribution of the same sample. There are a few large silver nanoparticles besides a large amount of small particles of size in the range of about 4 nm.

Figure 3(a–e) reflects TEM images of the silver nanoparticles derived from the template copoly(S-5MPEGA). The micrographs reveal that non-aggregative spherical

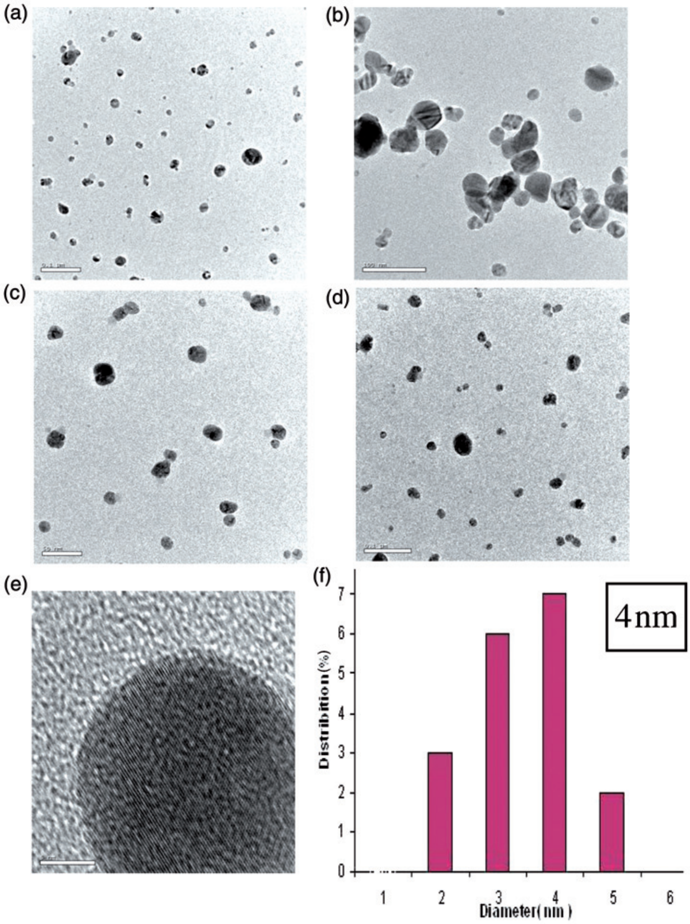

Figure 2. HRTEM micrographs of silver nanoparticles in copoly(S-7MPEGA). (a–e) Images recorded at different locations and (f) Histogram plot.

particles with a trace of rod-shaped particles are obtained. In Figure 3(f), the histogram shows the particle size of the silver nano in the range of 15 nm.

Figure 4(a–e) depicts the TEM images of the silver nanoparticles embedded from the template copoly(S-3MPEGA). Non-aggregative spherical particles with a trace of truncated triangular shaped particles are obtained. In Figure 4(f), the histogram shows the particle size of the silver nanoparticles in the range of 25 nm.

The copolymer not only functions as a stabiliser for the formation of silver nanoparticles but also serves as a ligand to form complexes with the silver ions. The acrylate copolymer serves as a nucleophile that can donate an electron pair into unoccupied orbital of the silver ions that exist on the surface. The unsaturated silver atom [11,12] is still co-coordinately bound to the copolymer. This co-ordination effect can substantially control the particle size. The particle size is found to be less the greater the chain length of the polymer, as the length of the polymer chain avoids the aggregation of

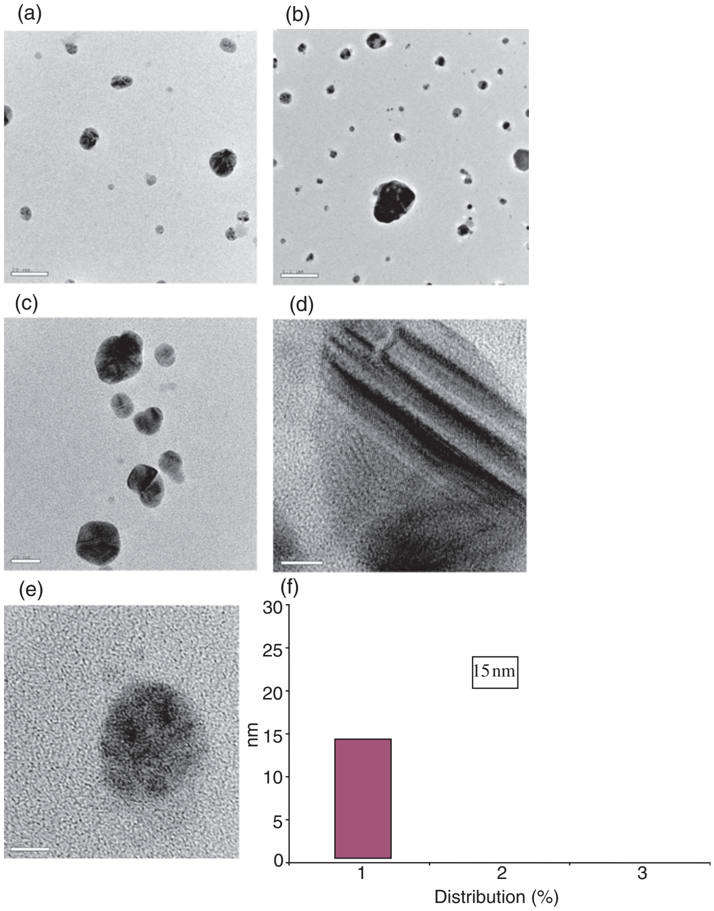

Figure 3. HRTEM micrographs of silver nanoparticles in copoly(S-5MPEGA). (a–e) Images recorded at different locations and (f) Histogram plot.

the particles by keeping them away from each other. Thus, silver ions are rapidly reduced to a silver atom [13] in a very short time by the solvent. The silver atom was still retained in the polymer. The microwave irradiation results in the decarboxylation of the biodegradable ester linkage in the polymer. This is a beneficial factor for the release of well-dispersed silver particles. A possible mechanism has been proposed for the formation of silver nanoparticles (Scheme 1). The size was determined to be of the nanometre scale by HRTEM. The proposed mechanism was also in accordance with the Norrish type II reaction that involves the decarboxylation of the ester linkage. To gain knowledge about the completion of the reduction process, UV-Vis spectra were taken.

3.2.2. *UV-Vis spectra*

Figure 5(a) shows the UV spectra of the copolymer-stabilised silver nanoparticles prepared by microwave heating of the 30 mg of the copolymer (five different compositions) with 10 mg of CH_3COOAg in 10 mL of the DMF solution for 60 s. Although DMF is capable

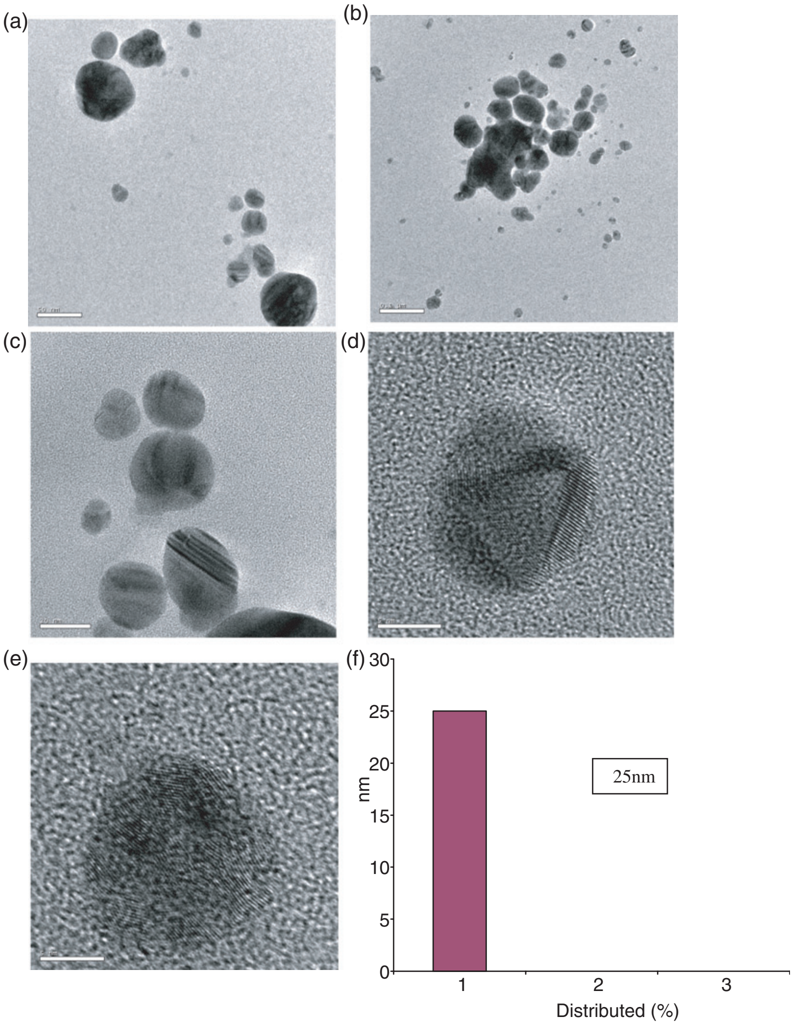

Figure 4. HRTEM micrographs of silver nanoparticles in copoly(S-3MPEGA). (a–e) Images recorded at different locations and (f) Histogram plot.

of reducing the silver ions to silver atoms at room temperature, the reduction rate is dramatically increased as the temperature is raised to the boiling point of the solvent used. Therefore, the growth of the metal particles cannot be controlled properly. Hence, a polymer capable of controlling the particle morphology is used as a protecting agent. A co-ordination is formed between the metal ion and the copolymer. Reduction of silver ion to silver atom takes place on the surface of the polymer. This controls the aggregation of the metal atoms in solution. The microwave heating after complex formation prevents the particle growth due to milder and uniform reaction conditions. This further prevents agglomeration of the metal particles and leads to the formation of monodispersed stable colloids. The surface plasmon resonance (SPR) band of the silver nanoparticles was observed around 420 nm. On the basis of Mie's theory, isotropic silver nanoparticles

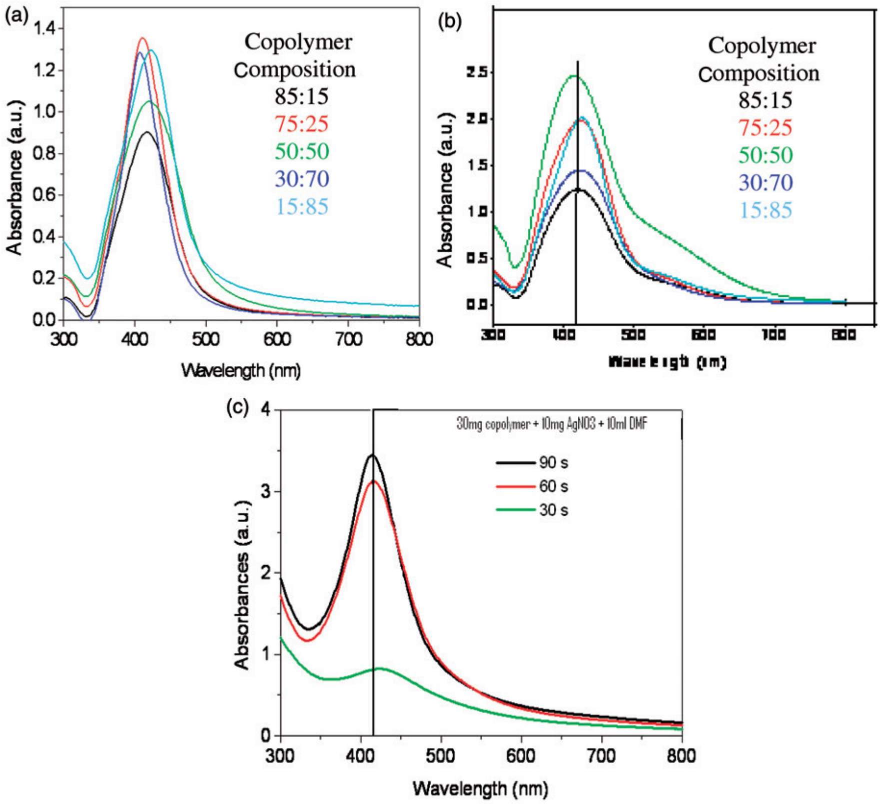

Figure 5. UV spectra of silver nanoparticles in copoly(S-7MPEGA). (a) Silver from silver acetate, (b) silver from silver nitrate, (c) different time intervals namely 30, 60 and 90 s.

of spherical shape would give a single symmetric absorption band around 420 nm, whereas anisotropic nanoparticles should exhibit two or more bands. A number of experiments have also proven this theory and given similar results [14–19]. Peaks around 300 nm, which are characteristic of silver ions, were found missing in the UV-Vis spectrum of the silver colloids obtained [20]. The presence of peaks around 420 nm confirms the formation of the silver nanoparticles. This indicates that all the silver ions are completely reduced. Confirmation of the complete reduction of silver ion to silver particles through UV-Vis absorption measurement is essential because it provides a deeper insight into the optical properties that depend on the size, distribution and the surface properties of silver nanoparticles.

Figure 5(b) shows the UV spectra of the silver nanoparticles prepared by microwave heating of the 30 mg of copolymer [five different compositions] with 10 mg of $AgNO_3$ in 10 mL of the DMF solution for 60 s. Although the surface plasmon resonance bands are observed at 420 nm, the absorption spectra are not similar to the profiles of the curves compared to that of silver acetate as shown in Figure 5(a). This is due to the high solubility of silver nitrate, which is indicative of the reduction taking place in the solution rather than on the surface of the copolymer template [21]. This means that the reduction may be fast enough that the polymer chains could not complex the silver ions and stabilise in an efficient manner. Hence, less sharp peaks are observed in the case of silver nitrate compared to silver acetate. Absence of peaks at 300 nm confirms the complete reduction of the silver ions to silver atoms. It is inferred that the silver colloid obtained in this system is monodispersed.

Figure 5(c) depicts the UV spectra of the silver nanoparticles obtained from 30 mg of copolymer (of composition 50 : 50) with 10 mg of CH_3COOAg in 10 mL of the DMF solution exposed to microwave heating for 30 s, 60 s and 90 s. The spectra illustrates that a more sharper and symmetrical peak is obtained when exposed to 90 s. This is because the rate of reduction of the silver ion to silver nanoparticle is enhanced when exposed to microwave heating for longer duration [22,23]. However, a resonance peak centred at 420 nm was observed irrespective of the exposure time to microwave heating.

Changing the copolymer, the weight of the copolymer and varying the solvent were performed in further analyses. The UV spectra were taken in all the cases under identical experimental conditions. In all the cases, the SPR band was obtained at 420 nm and the peak due to silver ion at 300 nm was found missing. All these results cumulatively suggest that the colloidal silver system so obtained was ideally monodispersed. This clearly shows that only silver nanoparticles are present in the colloidal dispersion. With ageing, the silver particles gradually aggregate to form a shiny silver film typically exhibiting 'metallic silver' reflectivity on the surface of the solution.

3.2.3. *FT-IR*

Peaks due to saturated ester at 1717 cm^{-1} observed in the polymer spectra are found missing in the nanoparticle spectra. This clearly shows that the ester linkage is easily degradable [24] under microwave irradiation. Presence of peaks due to aro.C =C bending (1667, 1580, 1500, 1452 cm^{-1}), aro.C–H str(3030cm^{-1}) and aro.C–H bending (952, 848, 719, 661 cm^{-1}) vibrations were observed. A possible mechanism is suggested in the reduction of silver ion to metallic silver (Scheme 2). The mechanism clearly suggests that the ester linkage of the polymer template is easily degradable under microwave irradiation thereby releasing silver particles of nanosize. Interactions of these silver nanoparticles with biosystems are just beginning to be understood.

3.2.4. *Antibacterial activity*

The antibacterial activity [25] of the silver nanoparticles dispersed in different copolymer matrices of different compositions were tested on genus *Bacillus* and *Staphylococcus aureus*. The preliminary results suggest that the silver nanoparticles dispersed in the different copolymer matrices copoly(S-7MPEGA), copoly(S-5MPEGA) and copoly(S-3MPEGA) show antibacterial activity. A higher reactivity towards the test organisms is observed when silver from silver nitrate is encapsulated in the polymer matrix in comparison to the silver derived from silver acetate. This is due to the greater solubility of silver nitrate in the polymer that favours the release of the silver nanoparticles readily. Hence, it is observed that the silver derived from silver nitrate is more bactericidal than the silver derived from silver acetate.

Among the three copolymer matrices, copoly(S-7MPEGA), copoly(S-5MPEGA) and copoly(S-3MPEGA), silver nanoparticles embedded in the copoly(S-7MPEGA) showed a higher reactivity towards the test organisms. The microorganisms upon treatment with silver ion resulted in cell death. The zone of lyses (mm) measured was maximum for silver nanoparticles embedded in the matrix copoly(S-7MPEGA) and minimum for silver nanoparticles embedded in the matrix copoly(S-3MPEGA). This was attributed to the minimum size of the silver nanoparticles (4 nm) particle in comparison to the size of silver nanoparticles (25 nm). Hence, the activity of silver nanoparticles in copolymer matrices is found to be of the order copoly(S-7MPEGA) > copoly(S-5MPEGA) > copoly(S-3MPEGA).

However, in a given set of copolymer matrix, the nanosilver encapsulated in different compositions did not alter the antibacterial activity towards the test organisms.

The antibacterial effects of a silver ion solution were investigated for *Staphylococcus aureus* and *Escherichia coli* by analysing the growth, morphology and structure of bacterial cells following treatment with the silver ion solution. Bacteria were exposed to the silver ion solution for various lengths of time, and the antibacterial effect of the solution was tested by Jung et al. [26]. The results suggest that silver ions may cause *S. aureus* and *E. coli* bacteria to reach an active but non-culturable (ABNC) state and eventually die.

In the report by Pal et al. [27], silver nanoparticles undergo shape-dependent interaction with the gram-negative bacterium *E. coli*. The interactions of silver nanoparticles with biosystems were beginning to be understood. Truncated triangular silver nanoplates displayed the strongest biocidal action, compared to spherical and rod-shaped nanoparticles and with Ag^+ (in the form of silver nitrate) and these particles are increasingly being used as microbicidal agents. It was speculated that silver nanoparticles with the same surface area but with different shapes might also have different effective surface areas in terms of active facets. Influence of the surface areas of different nanoparticles on their killing activity or the bacterial killing capacity of silver nanoparticles with the effective surface areas was not known. The results provide a basis for the measurement of shape dependent bacterial activity of silver nanoparticles.

In the present study, the microorganisms genus *Bacillus* and *S. aureus*, when exposed to silver ion solution, showed considerable changes in the cell membrane as a consequence of cell death. This was eventually measured by the zone of lyses as given in Table 3. On a comparative basis the shape of silver nanoparticles in different copolymer templates were analysed for the antibacterial activity.

(a) Ag/copoly(S-7MPEGA): Large number of nanospheres besides traces of less spherically symmetrical particles as observed through TEM images are shown in Figure 2. The antibacterial activity reported in Table 3 exhibits maximum cell death.
(b) Ag/copoly(S-5MPEGA): Large number of spherical particles with traces of plates as observed through TEM images are shown in Figure 3. The zone of lyses reported in Table 3 shows moderate antibacterial activity.
(c) Ag/copoly(S-3MPEGA): Large number of spherical particles with traces of truncated triangular prisms as observed through TEM images as in Figure 4. The zone of lyses reported in Table 3 shows minimum antibacterial activity.

However, the results observed are in contrast to the shape-dependent bacterial activity of AgNP as cited by Pal et al. According to their results, triangular nanoprisms exhibit strong biocidal activity in comparison to plates and spherical particles. The reverse trend

Table 3. Antimicrobial activity of silver nanoparticles against the different test organisms.

Copolymer matrices	Copolymer composition	Zone of lyses (mm) Silver from silver acetate *Staph aureus*	Zone of lyses (mm) Silver from silver acetate Genus *Bacillus*	Zone of lyses (mm) Silver from silver nitrate *Staph aureus*	Zone of lyses (mm) Silver from silver nitrate Genus *Bacillus*
Copoly(S-7MPEGA)	Five different copolymer composition	13	15	16	16
Copoly(S-5MPEGA)	Five different copolymer composition	12	14	15	15
Copoly(S-3MPEGA)	Five different copolymer composition	11	13	14	14

observed in the present study may be attributed to the trace amounts of truncated triangular prisms and plates instead of large quantity.

To conclude, the well-resolved silver nanoparticles of dimensions 4, 15 and 25 nm through polyol reduction method under microwave conditions exhibit excellent antimicrobial activity. Shape dependence of these nanosize particles on antibacterial activity is to be explored.

4. Conclusion

Synthesis of the polymer-stabilised silver nanoparticles in suitable solvents through chemical methods basically involves two processes: co-ordination of the metal ion to the polymer and the reduction of the metal ion to metal atom. Different polymers capable of complexing and stabilising the metal nanoparticles were synthesised by free radical technique. The GPC and TGA results confirm the lightweight and the stability of copolymers and these copolymers are used as a template for the synthesis of nanoparticles. After the complexation of the metal ion to the copolymer template, the reduction of metal ion to metal atom is efficiently performed under microwave irradiation. This prevents agglomeration and further particle growth of the metal atom. HRTEM and UV results provide further proof for the formation of silver nanoparticles with large number of spherical shape with dimensions of 4, 15 and 25. Silver nanoparticles of such dimensions are expected to have wide applications in various fields. The system is explored in their application as antibacterial material and found to be bactericidal. This methodology could also be applicable for producing other metal nanoparticles.

References

[1] H.H. Huang, X.P. Ni, G.L. Loy, C.H. CheW, K.L. Tan, F.C. Loh, J.F. Deng, and G.Q. Xu, *Photochemical formation of silver nanoparticles in poly(N-vinylpyrrolidone)*, Langmuir 12 (1996), pp. 909–912.

[2] Y.G. Sun and Y. Xia, *Shape-controlled synthesis of gold and silver nanoparticles*, Science 298 (2002), pp. 2176–2179.

[3] Y. Sun, Y. Yin, B.T. Mayers, T. Herricks, and Y. Xia, *Synthesis of gold microplates and polyhedral nanoparticles*, Chem. Mater. 14 (2002), pp. 4736–4745.

[4] A. Manna, T. Imae, K. Aoi, M. Okada, and T. Yogo, *Electrochemical of p-nitrophenol at supported mono- and bimetallic dendrimer encapsulated catalysis*, Chem. Mater. 13 (2001), pp. 1674–1681.

[5] Z. Zhang, R.C. Patel, R. Kothari, C.P. Johnson, S.E. Friberg, and P.A. Aikens, *Stable silver clusters and nanoparticles prepared in polyacrylate and inverse micellar solutions*, J. Phys. Chem. B 104 (2000), pp. 1176–1182.

[6] Z.P. Zhang and M.Y. Han, *One-step preparation of size-selected and well-dispersed silver nanocrystals in polyacrylonitrile by simultaneous reduction and polymerization*, J. Mater. Chem. 13 (2003), pp. 641–643.

[7] Q. Yang, F. Wang, K. Tang, C. Wang, Z. Chen, and Y. Qian, *The formation of fractal Ag nanocrystallites via γ-irradiation route in isopropyl alcohol*, Mater. Chem. Phys. 78 (2002), pp. 495–500.

[8] I. Capek, M. Riza, and M. Akashi, *Graft copolymers having hydrophobic backbone and hydrophilic branches, effect of temperature on the dispersion copolymerization of poly (ethylene glycol) macromonomer with styrene*, Angewandte Makromol. Chemie. 206 (1993), pp. 69–75.

[9] I. Capek, M. Riza, and M. Akashi, *Effects of the initiator type on the dispersion copolymerization of poly (ethylene glycol) macromonomer and styrene*, Polym. J. 24 (1992), pp. 959–970.

[10] I. Capek, M. Riza, and M. Akashi, *Dispersion copolymerization of methyl methacrylate and n-butyl acrylate copolymers*, J. Polym. Sci. Part A: Polym. Chem. 35 (1997), pp. 3131–3140.

[11] P. Mulvaney, P. Linnert, and A. Henglein, *Surface chemistry of colloidal silver in aqueous solution: observations on chemisorption and reactivity*, J. Phys. Chem. 95 (1991), pp. 7843–7846.

[12] V.V. Vukovic and J.M. Nedeljkopic, *Surface modification of nanometer-scale silver particles by imidazole*, Langmuir 9 (1993), pp. 980–983.

[13] A. Henglein and M. Giersig, *Formation of colloidal silver nanoparticles: Capping action of citrate*, J. Phys. Chem. B 103 (1999), pp. 9533–9539.

[14] Y. Sun, P. Mayers, T. Hericks, and Y. Xia, *Polyol synthesis of uniform silver nanowires: A plausible growth mechanism and the supporting evidence*, Nano Lett. 3 (2003), pp. 955–960.

[15] M. Mailerd, S. Giorgio, and M.P. Pileni, *Tuning the size of silver nanodisks with similar aspect ratios: Synthesis and optical properties*, J. Phys. Chem. B 107 (2003), pp. 2466–2470.

[16] R.C. Jin, Y. Cao, C.A. Mirkin, K.L. Kelly, G.C. Schatz, and J.G. Zheng, *Photoinduced conversion of silver nanospheres to nanoprisms*, Science 294 (2001), pp. 1901–1903.

[17] J.Q. Hu, Q. Chen, Z.X. Xie, G.P. Han, R.H. Wang, P. Ren, Y. Zhang, Z.L. Yang, and Z.L. Tan, *A simple and effective route for the synthesis of crystalline silver nanorods and nanowires*, Adv. Funct. Mater. 14 (2004), pp. 183–189.

[18] Y. Sun, P. Gates, B. Mayers, and Y. Xia, *Crystalline silver nanowires by soft solution processing*, Nano Lett. 2 (2002), pp. 165–168.

[19] T. Ung, L.M. Liz-Marzan, and P. Mulvaney, *Controlled method for silica coating of silver colloids influence of coating on the rate of chemical reactions*, Langmuir 14 (1998), pp. 3740–3748.

[20] M. Chen, L.-Y. Wang, J.-T. Han, J.Y. Zhang, Z-Y. Li, and D.-J. Qian, *Preparation and study of polyacryamide-stabilized Silver nanoparticles through a one-pot process*, J. Phys. Chem. B 110 (2006), pp. 11224–11231.

[21] I. Pastoriza-Santos and L.M. Liz-Marzan., *Formation of PVP-protected metal nanoparticles in DMF*, Langmuir 18 (2002), pp. 2888–2894.

[22] I. Pastoriza-Santos and L.M. Lis-Marzan, *Formation and stabilization of silver nanoparticles through reduction by N, N-Dimethylformamide*, Langmuir 15 (1999), pp. 948–951.

[23] I. Pastoriza-Santos, C. Serra-Rodriguez, and L.M. Liz-Marzan, *Self-assembly of silver particle monolayers on Glass from $Ag+$ solutions in DMF*, J. Colloid Interface Sci. 221 (2000), pp. 236–241.

[24] J.A. Mikroyannidis, *Photocrosslinkable oxopenta-[1,4-dienyl]phenyl-2-25. Photocrosslinkable polymers based on 4-[5-(4-hydroxyphenyl)]-3-methacrylate: Photocrosslinking studies and reactivity ratios with vinylcyclohexane*, Eur. Polym. J. 24 (1988), pp. 1093–1099.

[25] A. Arun and B.S.R. Reddy, *Polymeric drug for antimicrobial activity studies: Synthesis and characterization*, J. Bioact. Compat. Polym. 18 (2003), pp. 219–228.

[26] W.K. Jung, H.C. Koo, K.W. Kim, S. Shin, S.H. Kin, and Y.H. Park., *Antibacterial activity and mechanism of action of the silver ion in* Staphylococcus aureus *and* Escherichia coli, Appl. Environ. Microbiol. 74 (2008), pp. 2171–2178.

[27] S. Pal, Y.K. Tak, and J.M. Song, *Does the antibacterial activity of silver nanoparticles depend on the shape of the nanoparticle? A study of the gram-negative bacterium* Escherichia coli, Appl. Environ. Microbiol. 73 (2007), pp. 1712–1720.